Mem. S.A.It. Suppl. Vol. 16, 22

Memorie della
Supplementi

The ISA accelerometer for BepiColombo mission

V. Iafolla, E. Fiorenza, C. Lefevre, S. Nozzoli, R. Peron, A. Reale, and F. Santoli

Istituto Nazionale di Astrofisica – Istituto di Fisica dello Spazio Interplanetario, Via del Fosso del Cavaliere, 00133 Roma, Italia
e-mail: valerio.iafolla@ifsi-roma.inaf.it

Abstract. The Italian Spring Accelerometer (ISA) will give a fundamental contribution to the Radio Science Experiments of BepiColombo mission, enabling substantial improvement of the knowledge of Mercury's orbit and rotation, and of the relativistic dynamics in the solar system. ISA is a three–axis accelerometer devoted to the measurement of the non–gravitational acceleration of Mercury Planetary Orbiter (MPO), whose knowledge is important in order to fully exploit the quality of the tracking data. ISA shall have an intrinsic noise level of $10^{-9} m/s^2/\sqrt{Hz}$ in the $3 \cdot 10^{-5}$ Hz to 10^{-1} Hz frequency range, to guarantee the fulfilment of the RSE scientific goals. A comprehensive presentation of ISA accelerometer is given, including details about its scientific and technological features, the updated measurement error budget, the ongoing experimental activities and foreseen calibration and science operations strategies.

Key words. Solar system – Mercury – Accelerometers – Non–gravitational perturbations – Gravimetry – General relativity

1. Introduction

The **Radio Science Experiments** (**RSE**) constitute an important set among the experiments which will be performed by the forthcoming BepiColombo mission (Anselmi & Scoon, 2001; Benkhoff et al., 2010). By radiometric tracking of the Mercury Planetary Orbiter (MPO) spacecraft[1], precise measurements of

- gravitational field of Mercury
- rotation of Mercury
- general relativistic effects, in particular Mercury perihelion precession

will be performed. The overall procedure is fairly complex (Milani et al., 2001, 2002; Milani & Gronchi, 2010). The tracking data will be used together with a dynamical model for spacecraft and Mercury motion in an orbit determination and parameter estimation procedure, in order to extract from the data themselves the sought–for information. The dynamical model is based on general relativity (at the relevant Post–Newtonian level) for the motion of bodies in the solar system and on a spherical harmonics expansion of the Hermean gravitational field, in order to determine accurately the MPO motion around Mercury. The models will depend in general on a set of parameters which will be estimated during orbit determi-

Send offprint requests to: V. Iafolla

[1] The BepiColombo mission is composed of two spacecraft, the Mercury Planetary Orbiter and the Mercury Magnetospheric Orbiter (MMO), characterised by different scientific objectives and different orbital configurations around Mercury.

nation; among them, the quantities of interest, such as the PPN parameters and the spherical harmonics coefficients C_{lm} and S_{lm} of Mercury gravity field.

A distinctive feature of BepiColombo with respect to other deep–space missions is its relative proximity to the Sun. This has two fundamental consequences. First, general relativistic effects are enhanced (motion near a massive body). Second, the harsh environment the spacecraft will move in: non–gravitational effects due to surface forces, mainly the solar radiation pressure, perturb the motion of the spacecraft and mix with the gravitational effects. These forces are very difficult to model, since they depend in a complex way on incoming radiation and spacecraft surface optical properties and spacecraft attitude (Lucchesi & Iafolla, 2006). Analitical models do indeed exist, but they are effective only in particular cases. This is a serious problem, since it limits the accuracy with which the relativistic and geophysical parameters could be recovered. In order to overcome it, an accelerometer onboard the MPO — the **Italian Spring Accelerometer** (**ISA**) — will directly measure the non–gravitational perturbations so as to precisely take them into account in the orbit determination and make the MPO an *a posteriori* drag–free spacecraft.

The use of high–performance accelerometers instead of analytical or numerical models, in order to improve the quality of orbit determination and parameter estimation, has been given increasing attention in recent years. Indeed, the performance of the tracking systems has been steadily improving, whereas this cannot be said about modelization. Examples of the accelerometers effectiveness are given by the CHAMP and GRACE geodetic missions, where the precise GPS position measurements are combined with accelerometric measurements (see van den Ijssel & Visser, 2007; Bruinsma et al., 2003; Flury et al., 2008). The use of acceleration data improves the geophysical parameters estimation and is far better than the use of empirical acceleration terms in the modelization; these empirical accelerations could in fact improve the quality of the fit (post–fit RMS reduction), but at the cost of a predictivity lack (no or small correlation with physically relevant parameters).

The ISA accelerometer characteristics requirements for BepiColombo mission follow from the BepiColombo RSE requirements (see Iafolla & Nozzoli, 2001; Iafolla et al., 2010). As discussed in Benkhoff et al. (2010), the MPO spacecraft will be three–axis stabilised, Nadir pointing, characterised by a 400×1500 km polar orbit around Mercury. This orbit configuration is suitable for the recovery, with a signal–to–noise ratio larger than 10, of Mercury's gravity field up to degree $l = 25$, corresponding to a spatial resolution of about 300 km on the surface of Mercury (Milani et al., 2001, 2002). In order to reach the goals of the RSE, the orbit must be known with an accuracy of at least 1 m in the along–track direction over one orbital revolution of the MPO around Mercury, i.e., over 8355 s. This corresponds to an along–track acceleration accuracy of about 10^{-8} m/s^2. Therefore, this number has been considered equivalent to the acceleration measurement error over the typical arc length.

The requirement of a noise level of 10^{-8} m/s$^2/\sqrt{Hz}$ (spectral density), however, is not necessary for all frequencies inside the accelerometer's band. Indeed, as shown in Fig. 1, which describes the noise contributions due to the accelerometer and to the tracking system, at low frequency the noise is dominated by the thermal disturbing effects at the interface between spacecraft and accelerometer while at higher frequencies the noise is dominated by the tracking errors. The red line represents ISA intrinsic noise; the green line represents the filtered thermal noise effects due to a possible white noise at a level of 4°C$/\sqrt{Hz}$, which may be present at the mechanical interface between the spacecraft structure and ISA; the blue line represents the equivalent acceleration associated to the Doppler noise; finally, the black line represents the total noise (quadratic sum of the previous uncorrelated noise sources). The various noise sources — ISA intrinsic noise, thermal noise, tracking noise — constrain the ISA sensitivity requirement (diamond line). It is clear the need to fully exploit the accelerometer performances only in a narrower frequency band, between 10^{-4} Hz and 10^{-3} Hz. We stress that these results have been obtained in the case of a passive thermal control. Currently, an active thermal control is foreseen as baseline; the thermal effects will be further attenuated by a factor 700. In Table 1 the main RSE–derived requirements are summarized.

2. The accelerometer

ISA (Iafolla & Nozzoli, 2001; Iafolla et al., 2010) is a three–axis accelerometer, characterised by high sensitivity and a wide frequency bandwidth. Its configuration for BepiColombo is based on two units: the **ISA Detector Assembly** (**IDA**) (see Fig. 2) and the **ISA Control Electronics** (**ICE**). IDA contains the three detector units, the preamplifier and the analog–to–digital conversion section, while ICE contains the remaining control electronics and is the interface with MPO Data Management System (DMS). The main characteristics of the instrument are shown in Table 2.

Each of the three sensing elements — which are the core of the instrument — is constituted by three main parts:

- mechanical oscillator
- actuation and control
- signal detection.

A rendering of the mechanical oscillator is shown in Fig. 3. A capacitor transducer in a bridge configuration, followed by a low–noise amplifier, provides the detection of the signal. The bridge is biased at frequency f_p = 10 kHz and accelerations at frequency f_s, acting on the proof mass, cause an unbalance of the capacitive bridge and a modulation of the bias voltage: at the output of the capacitive bridge the signal is seen at the two side bands, $f_\pm = f_p \pm f_s$. Transferring the signal to high frequency allows the amplifier to work at a frequency (10 kHz), where its temperature noise is lower, avoiding its $1/f$ noise. The other important characteristic of the mechanical oscillators, besides their resonance frequency, is the mechanical quality factor Q_m. A value of ~ 1 is sufficient, in our case, to make the Brownian noise contributions negligible. The transducer must have a high electromechanical coupling factor β (ratio between the mechanical energy of the oscillator and the electric power to be measured). The elements of the accelerometer must be stable in time and independent from the variation of temperature. Depending on the thermal sensitivity of the accelerometer, a spurious signal arises if a temperature change occurs; the instrument thermal control acts to keep the temperature variations as low as possible, in order to avoid spurious effects exceeding the required sensitivity in the instrument frequency band.

The accelerometer has an intrinsic noise of 10^{-9} m/s$^2/\sqrt{Hz}$ in the frequency band of $3\times10^{-5}-10^{-1}$ Hz. As described in Milani et al. (2001), the typical arc length [2] will be about 8 h. Therefore, this value has been assumed as the lower limit of the accelerometer band (about 3×10^{-5} Hz). The upper limit for the band is dictated by the requirement of a linear response of the accelerometer to a given perturbation. This means that the accelerometer must be used in a frequency region where its transfer function is flat, i.e. below the oscillator resonance frequency.

The measurement total noise, intrinsic plus induced by the spacecraft, is equal to 10^{-8} m/s$^2/\sqrt{Hz}$; this means that integrating over a time Δt the accelerometer performance can be much better than 10^{-8} m/s^2, that is the accuracy required by the RSE for the MPO orbit reconstruction. Several sources of error have to be added to the intrinsic noise of the instrument. These are addressed in Section 4. Here we notice that thermal effects play an important role. In fact, each sensing element is affected by possible temperature variations in its surrounding environment, which produce a spurious acceleration signal (see Section 4). The thermal environment the MPO will face will be characterized by noticeable variability that will re-

[2] Between 4 and 12 h depending on the visibility conditions. The visibility conditions constrain the way in which the data are collected in the case of range and range–rate measurements, which will not be continuous.

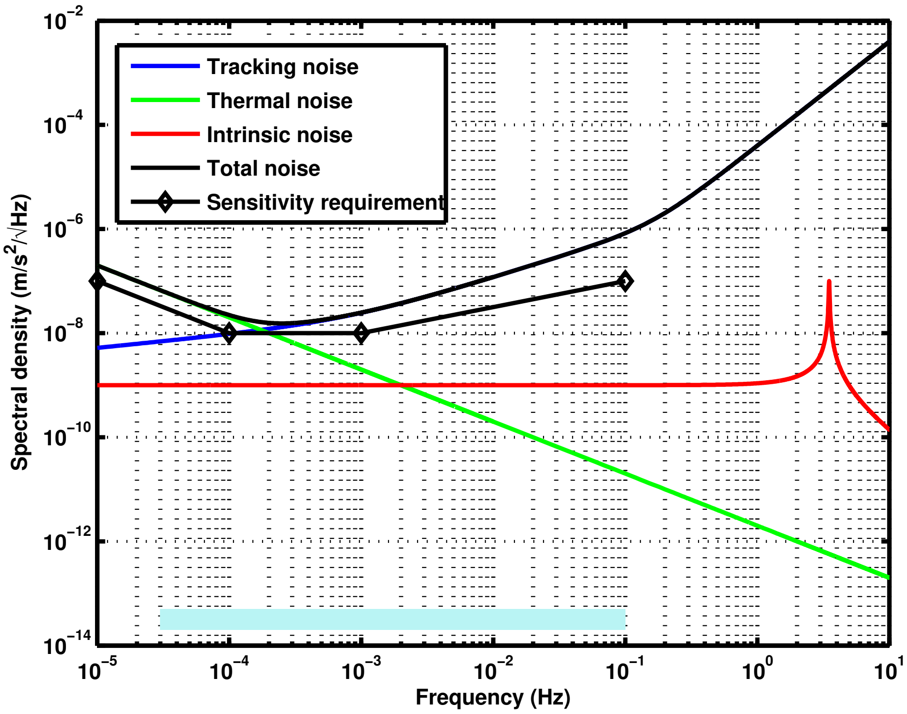

Fig. 1. Noise contributions from the accelerometer and the tracking system as used in the simulations that have been performed to prove the reliability of the RSE. The total noise level is mainly due to the thermal effects on the accelerometer at low frequencies and to the tracking noise at high frequencies. The light blue bar represents the ISA frequency band.

Table 1. RSE–related features and performances.

Parameter	Value
Measurement Frequency Range	$3 \times 10^{-5} - 10^{-1}$ Hz
Maximum expected signal	3×10^{-6} m/s^2
Measurement total noise	10^{-8} m/s^2/ $\sqrt{Hz}$
Instrument intrinsic noise	10^{-9} m/s^2/ $\sqrt{Hz}$
Required measurement accuracy	10^{-8} m/s^2
Readout interval	1 s

sult in temperature variations estimated to be 4°C per orbit and 25°C per Mercury year for IDA, at the spacecraft/instrument interface. In order to overcome this problem, apart from isolation layers, an active thermal control system has been designed; currently its performance guarantee a reduction of the thermal variation of a factor 700.

3. Measurement concepts

The accelerometer task is the direct measurement of surface, non–gravitational accelera-

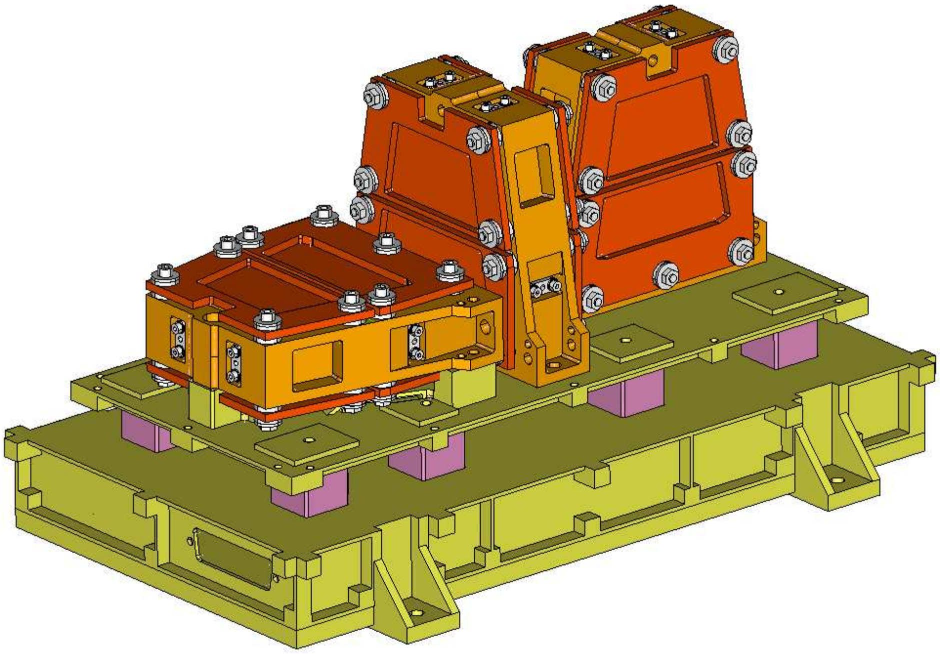

Fig. 2. The core of ISA Detector Assembly (IDA): the three sensing elements mounted on a common baseplate.

tions acting on the spacecraft. One can identify at least three different types of perturbations due to electromagnetic radiation impinging on the spacecraft surfaces:

– Visible radiation coming directly from the Sun (**direct solar radiation pressure**)
– Visible radiation from the Sun being reflected by the surface of Mercury (**albedo radiation pressure**)
– Infrared radiation emitted from the surface of Mercury.

The ISA accelerometer will measure the combined effect of all of them on the MPO spacecraft. In Lucchesi & Iafolla (2006), the effect of the first two types of perturbations has been studied, and the advantages of using on–board accelerometer data with respect to models of the non–gravitational perturbations have been shown.

The acceleration measurements are used in the orbit determination, instead of analytical or numerical modeling. In this respect, accelerometric measurements are on a different footing with respect to tracking data: they are part of the modelisation setup, rather than of the data themselves. The usual procedure implies writing the equations of motion for a reference point of the spacecraft, which is usually its center of mass (COM). The equations of motion must include the various forces acting on the spacecraft, and therefore also the non–gravitational ones, which are provided by the ISA measurements, in the BepiColombo case. An ideal accelerometer would be one with all three elements in the spacecraft COM. ISA is however composed by three different elements (each of them measuring the acceleration acting on a definite direction), and at most one of the three can be placed in the COM. Operational constraints can in any case prevent any one of them to be placed in such a position.

In general, the measurement of an accelerometer (whatever its position) is described by:

$$\boldsymbol{A}_{meas} \simeq \boldsymbol{B} + S_f \boldsymbol{A}_{true} + \boldsymbol{A}_{noise}, \quad (1)$$

Table 2. ISA characteristics. These are divided in mechanical, physical, power and thermal characteristics.

Parameter	Value
Mechanical	
Proof masses	0.2 kg
Resonance frequency	3.5 Hz
Mechanical quality factor	10
Physical	
Mass (total)	5.8 kg
Dimensions (IDA)	300 × 170 × 180 mm
Dimensions (ICE)	170 × 130 × 86 mm
Power	
Electronics power dissipation (without heather)	7.4 W
Total Average power dissipation with heather and in worst case condition	10.1 W
Total Peak power dissipation with heather and in worst case condition	12.1 W
Thermal	
IDA Operative range	0;+40 °C
IDA Non Operative range	-10;+55 °C
IDA I/F Orbital stability	+/-2 °C/orbit
IDA I/F sidereal stability	+/-12.5 °C/Mercury year
ICE Operative range	-20;+50 °C
ICE Non Operative range	-40;+60 °C
Sensor Heads temperature sensitivity	5×10^{-7} m/s^2/°C
Front End Electronics temperature sensitivity	5×10^{-8} m/s^2/°C

where $\boldsymbol{A}_{meas}$ and $\boldsymbol{A}_{true}$ are the measured acceleration and the true acceleration, which are affected by a bias $\boldsymbol{B}$ and a scale factor S_f (omitting possible non–linear contributions), and $\boldsymbol{A}_{noise}$ is the contribution due to stochastic and deterministic noise. In a generic position, the signal sensed by each element contains not only the part due to non–gravitational effects, but also spurious parts. Indeed, the true acceleration acting on each ISA sensing element can be written as

$$\boldsymbol{A}_{true} = \boldsymbol{a}_{TID} + \boldsymbol{a}_{APP} - \boldsymbol{a}_{NGP} \quad (2)$$

where $\boldsymbol{a}_{TID}$ is the contribution of the gravity gradients

$$\boldsymbol{a}_{TID} = T\boldsymbol{R} \quad T_{ij} = \frac{\partial^2 V}{\partial x_i \partial x_j}, \quad (3)$$

$\boldsymbol{a}_{APP}$ the contribution of the apparent accelerations

$$\boldsymbol{a}_{APP} = -\omega\times(\omega\times\boldsymbol{R}) - \dot{\omega}\times\boldsymbol{R} - 2(\omega\times\dot{\boldsymbol{R}}) - \ddot{\boldsymbol{R}}, \quad (4)$$

where V is the gravitational potential of the primary (i.e. Mercury), $\boldsymbol{R}$ the position vector of each proof mass with respect to the spacecraft center of mass, $\boldsymbol{\omega}$ the spacecraft angular velocity[3]; $\boldsymbol{a}_{NGP}$ represents the part due to the non–gravitational perturbations, i.e. the goal of ISA measurements. We can notice that both $\boldsymbol{a}_{TID}$ and $\boldsymbol{a}_{APP}$ terms depend on the position vector $\boldsymbol{R}$. Therefore, a position different from the spacecraft COM implies a spurious signal which has to be properly accounted for in order to obtain the correct acceleration measurements. The position vector $\boldsymbol{R}$ has turned out to be the most critical parameter; due to high–gain antenna (HGA) and solar panel movements, and also to fuel consumption and slosh-

[3] The spacecraft attitude is measured by its Attitude and Orbit Control System (AOCS), and is considered as “given” for our purposes.

Fig. 3. ISA sensing element. Three of these elements are arranged with the electronics to compose the ISA three–axis accelerometer.

ing, its time–variable position could not be determined with the required accuracy (the corresponding part of the spurious signal therefore adds to the total noise of the acceleration measurement).

An alternative and effective solution has been found, in the context of BepiColombo mission definition[4]. The choice of spacecraft COM as the reference point, with respect to which to write the equations of motion, is the usual one, but is not unique. These equations can be written for whatever point of the spacecraft; the important thing — with regard to the mission scientific objectives — is that these equations contain the parameters related to the dynamics the spacecraft is subject to (i.e., Hermean gravity field harmonics, PPN parameters and so on), so that these parameters could be estimated during orbit determination. Instead of writing the equations of motion of spacecraft COM, and referring to them both accelerometer *and* tracking measurements (the phase center of HGA is also out of the COM), the equations of motion of the accelerometer can be written[5], referring the tracking measurements *directly* to it. It turns out that the new equations of motion do not depend on the COM position, thereby nulling an important source of error (see Milani & Gronchi, 2010).

[4] Following mainly a proposal by H.-R. Schulte of EADS Astrium.

[5] In fact, due to the finite dimensions of the accelerometer, a particular point of it has to be chosen to represent the instrument. Currently, this is the ISA vertex, a geometrical point fixed with respect to IDA Unit Reference Frame, and located in the design position of central sensing mass center of mass. Therefore, the signals have to be properly reduced to this point.

4. Error budget

The assessment of the measurement error is fundamental to fix the requirements on the spacecraft/instrument interface and for the relative assessment of the data products in the overall RSE procedure. The various sources of uncertainty in the measurement can be broadly divided in two categories, based on their spectral content: *periodic* or *pseudo–sinusoidal* and *random*[6]. They have to be compared with the requirements coming from RSE (see Table 1); to this end, two quantities are defined, the measurement accuracy $A_0 = 10^{-8}$ m/s^2 and the measurement noise (spectral density) $S_0 = 10^{-8}$ m/s$^2/\sqrt{Hz}$.

It has to be remarked that the construction of the error budget has a two–fold meaning. On one side, it has the purpose of assessing the effects on the experiment uncertainty and evaluating their relative contribution, in order to guarantee the fulfilment of the RSE objectives. On the other side, it establishes the requirements to put on the overall spacecraft environment (attitude, microvibrations, and so on).

The current measurement error budget for nominal observations mode is summarized in Table 3. It refers to the new concept of RSE measurement and therefore differs from the previous estimates, as in Iafolla et al. (2010) (see also Iafolla et al., 2007). For each error source, the corresponding effect is shown, together with the estimates of periodic and random errors.

The acceleration disturbances are due to mechanical noise at the MPO/instrument interface and to residuals in the data reduction procedure. The mechanical noise is caused by the vibrations of MPO structural and moving (e.g., HGA and the solar panel) parts. Requirements have been put on it, in order to limit the spurious noise that would bias the signal and especially to avoid signal power nearby the resonance frequency of the mechanical oscillator (which would drive the accelerometer outside its dynamics). The data reduction residuals are related to the reconstruction of the acceleration vector at ISA vertex. This implies removing from the signal the contributions of gravity gradients and apparent accelerations, as described by Eqs. 3 and 4 respectively.

An important consequence of the new concept of RSE measurement is that $\boldsymbol{R}$ does not represent anymore the distance between each proof mass and the spacecraft COM, but the distance between each proof mass and the instrument vertex; this latter distance is not only smaller than the former one, but is also better known (depending on the well–known accelerometer geometry). The resulting error term has therefore a reduced magnitude with respect to the previous estimate: it depends only on knowledge of the sensing axes directions with respect to an inertial frame (MPO attitude) and of the sensing elements positions (ISA geometry). It is important to notice that this contribution to the error budget comes only from those spurious signals which cannot be reliably removed *a posteriori* from the accelerometer measurements. The spurious signal removed in the data reduction is much larger; for an appropriate operation of the accelerometer, it needs only not to exceed the dynamic range of the instrument[7]. The overall contributions to the error are 55 % A_0 and 90 % S_0.

Thermal variations at the spacecraft/instrument interface will cause a spurious signal of the accelerometer output. The most sensitive part of the instrument (sensing head mechanics) has a thermal sensitivity of $5 \cdot 10^{-7}$ m/s^2/°C. This means that a temperature

[6] The periodic error sources are mainly at the MPO mean motion frequency n or its harmonics. We have to underline that the listed phenomena can cause effects also at other frequencies outside the band of the instrument (as is the case for thermal effects), but these are not relevant (apart from possible long–term stability issues). The random error sources have effects which are not characterized by definite frequencies, but are instead spread over the entire instrument band.

[7] It has to be remarked that the accelerometer is also subject to inertial accelerations related to the linear (rigid body) motion of the MPO, due to change in its configuration and then to its COM displacement (last term on the right–hand side of Eq. 4). These accelerations are however acting also on the HGA; therefore they are automatically accounted for in the new RSE concept and their contribution to the error budget vanishes.

Table 3. ISA measurement error budget for nominal observations mode. See the text for the explanation of the various terms.

Error term	**Origin of the perturbation**	**Periodic error (% A_0)**	**Random error (% S_0)**
Acceleration disturbances	MPO generated mechanical noise Data reduction residuals	55	90
Thermal effects	ISA sensitivity to external temperature variations	15	30
Calibration errors	ISA calibration errors	10	Negligible
ISA internal errors	ISA intrinsics noise Non–linearity Crosstalk	10	10
	ISA sensitivity to out–of–band accelerations	10	30
Totals		100	100

variation of 1 °C gives a spurious acceleration signal equal to $5 \cdot 10^{-7}$ m/s^2. Taking into account the maximum foreseen temperature variation inside the instrument bandwidth (2 °C peak, at the MPO orbital period around Mercury) and the attenuation factor of 700, a value of 15 % A_0 for the periodic part is obtained. A similar calculation for the random part, with a thermal noise of 4 °C/$\sqrt{Hz}$, gives a value of 30 % S_0.

The calibration procedures, described in Section 6, bring in an error in the measurement, due to the uncertainty in the recovered parameters. This error has been estimated as 10 % A_0 for the periodic part and negligible for the random one.

The instrument itself introduces an uncertainty due to its internal working. A series of processes — Front End Electronics noise, Brownian noise, dissipation in damping resistors and so on — contribute to ISA intrinsic noise. Non linear terms (neglected in Eq. 1) contribute to $\boldsymbol{A}_{meas}$. Each sensing element could pick up signal from directions orthogonal to its proper one, due to crosstalk phenomena (internal coupling of different modes). All this sources sum up to 10 % A_0 for the periodic part and 10 % S_0 for the random one. These values are consistent with experimental measurements of ISA noise level done in a differential configuration (see Section 5). To these it has to be added the sensitivity of the instrument to accelerations outside its band. This further contribution has been estimated as 10 % A_0 (periodic part) and 30 % S_0 (random part).

5. Experimental activities

The development of the instrument relies on a strong ensemble of laboratory experimental activities. These are aimed at testing the various technological solutions on prototypes, measuring the various characteristics (see Table 2), testing selected effects, doing performance checks on bread–boards built by the industrial contractor. The main tasks — described in the following — concern tests on thermal control system and measurements of the intrinsic noise level of the instrument (using **common–mode rejection**); activities are also devoted to the development of the read–out electronics and an important role is performed by tests on bread–boards built by the industrial contractor. Finally, as fundamental part of these activities, the very delicate on–ground calibration procedures are foreseen (see Section 6).

An important test to be performed on the instrument is the check of its sensitivity, which is identified with the instrument intrinsic noise. Such a test is difficult in a laboratory environment, mainly due to seismic noise: the seismic noise is indeed higher than the instrument sensitivity (10^{-9} m/s^2/$\sqrt{Hz}$), and it is not possible to distinguish it from the noise produced by the instrument itself.

A way to overcome this difficulty is to arrange two equal accelerometers in a differential configuration: the two sensing elements are mounted rigidly one with each other, so that their sensing axes are parallel. The seismic signal acts the same way for the two elements (common–mode) and can be rejected by subtracting one element output from the other, thereby leaving the noise coming from the elements themselves. The result of such a procedure can be seen in Fig. 4, where the power spectral density of the two output and that of their difference ("Rejection") is shown. The rejection is taken as the upper limit of the single elements intrinsic noise. The noise coming from the environment is about two orders of magnitude higher than the noise coming from the instruments. This result thus confirms that the instrument achieves the required level of performance.

It has been performed a series of tests on two bread–boards of the sensing element provided by the industrial contractor. These two bread–boards are representative of flight version (at current desing status), apart from mass suspension elements (for one of the two, replaced by a rigid part) and sensing heads feet. These tests aimed mainly at checking the compatibility of the bread–boards with the requirements on sensing elements. Among the various tests, we want to underline here the thermal sensitivity tests and the measurement of the transfer function in vacuum (see Fig. 5). It has to be noted that this measurement has been done under the local Earth gravity; this condition increases the system resonance frequency.

6. Instrument calibration

For "calibration" we mean the series of procedures and measurements that define all the instrument characteristics, in all the phases and operative conditions, and enable a complete and precise reconstruction of the measured signal. In this wider meaning, calibration includes the data reduction procedure of the three sensing elements output in order to obtain the acceleration signal at ISA vertex. We can divide these procedures in three steps, briefly explained in the following.

The first step includes the tests necessary to characterize the instrument itself. The list of quantities to be measured and features to be verified includes:

- transfer function
- transducer factor
- linearity of response
- intrinsic noise
- thermal stability.

These are planned to be performed on ground; some of them will be repeated in the various phases of the mission, to verify that the instrument works properly, with the declared performance.

The second step is related to calibration in the strict meaning, i.e. determination of:

- transducer factor
- electromechanical actuation factor
- sensing axes directions
- sensing elements positions.

The calibration of the transducer factor relates the output of the capacitive bridge to the measured acceleration; it is planned to be performed throughout the entire mission. The transducer factor measurement is strictly related to the quality of the final data product, and various strategies have been studied to perform it. The baseline is to use the ISA actuators to give each proof–mass a known (electric) acceleration, and then obtain the transducer factor by comparing this input with the corresponding output. Another (backup) possibility is to perform some MPO manoeuvres at selected times and by a precise knowledge of the spacecraft attitude (given by the AOCS), calculate the corresponding acceleration on each sensing element and then again the transducer factor. A further opportunity will be available in the cruise phase, during the Superior Conjunction Experiment (SCE) (see Milani et al., 2002). In that phase of the mission the Mercury Composite Spacecraft (MCS)[8] will travel in a relatively stable dynamic environment (far from the Sun and with constant attitude) in such a way that the non–gravitational perturbations acting on the MCS

[8] During the long cruise, MPO and MMO will travel together, thrusted by solar electric propulsion.

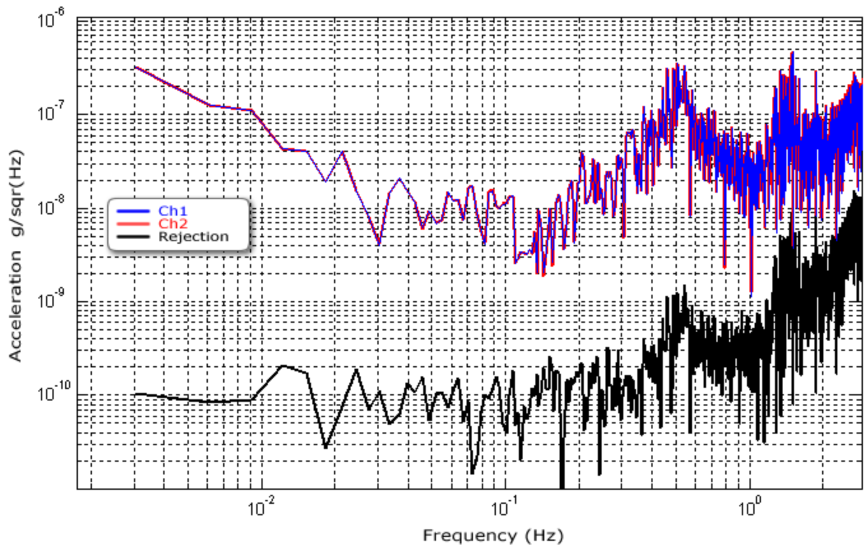

Fig. 4. Rejection test with two equal sensing elements, mounted rigidly with their sensing axes parallel. The power spectral density of the two instrument output is shown, together with that of their difference.

will be nearly constant; high–precision tracking will be also performed. The comparison of accelerometer with tracking data will enable at least in principle a calibration of the accelerometer. In order to perform the baseline calibration with actuators, the electromechanical actuation factor must be known *a priori*. This further, fundamental, calibration will be performed in laboratory, before the instrument integration on the spacecraft. Moreover, the directions of the sensing axes and the positions of the sensing elements must be precisely known in order to reconstruct the acceleration signal. While the positions will be reliably known by design, the directions will have to be determined by a dedicated laboratory procedure, which is currently under development.

The third, final, step includes the data reduction procedure. It gathers all the relevant data (from the second step and using also ancillary data, e.g. spacecraft attitude) and combines them to obtain the ISA scientific product, i.e. the three components of the acceleration acting on ISA reference point (ISA vertex), including the correction for the residual spurious signals related to the internal shift from the sensing elements to the vertex (see Eqs. 3 and 4).

7. Scientific operations

During the long time span of BepiColombo cruise and nominal (and possibly extended) mission, ISA will have many opportunities of contributing to the overall activities. Its baseline is the high–quality measurement of non–gravitational perturbations acting on MPO, to be provided to the orbit determination and parameter estimation procedure, in order to exploit as much as possible the tracking data information content. This role has been recently enriched with the new RSE concept (discussed in Section 3), making the accelerometer reference point the virtual test mass freely floating around Mercury. Other scientific possibilities lie in the long cruise phase, with its very–low–noise environment: apart from the envisaged calibrations (discussed in Section 6),

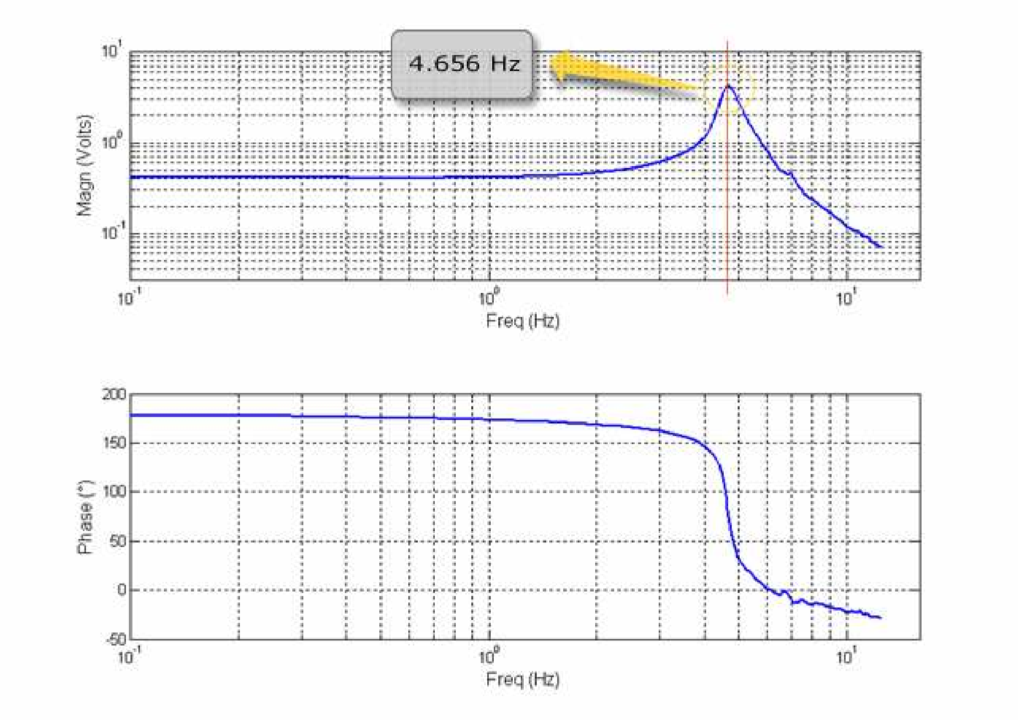

Fig. 5. The transfer function measured for a bread–board of the sensing element, amplitude (upper part) and phase (lower part).

there is the possibility of performing fundamental physics tests, especially during the various flybys (around Earth, Venus and Mercury) necessary for inserting the spacecraft in its proper orbit around Mercury.

In order to cope with the different needs of the various mission phases, the instrument is set up following a number of Scientific Operative Modes, which currently are:

- **Nominal Observations.** The nominal way of working, with internal parameters set up accordingly
- **Internal Calibration.** Calibration procedure with internal actuators to be performed periodically (see Section 6)
- **Calibration with MPO manoeuvres (backup).** Additional calibration procedure using MPO manoeuvres (see Section 6)
- **High–frequency Observations.** Data sampling at high frequency, for out–of–band noise monitoring.

The raw data, filtered and decimated on–board, are then sent to Earth. Before being used in the orbit determination and parameter estimation procedure, though, they have to be preprocessed, i.e. calibrated. The procedures to perform this task are currently being developed, to be included in the overall ESA data processing pipeline.

8. Conclusions

BepiColombo is an ambitious Solar System exploration mission, which will contribute to the study of planet Mercury and of the inner Solar System environment, and to fundamental physics. In particular, the set of the Radio Science Experiments will improve substantially the knowledge of Mercury internal structure and composition, and it will test the general relativity theory. The Italian Spring Accelerometer will have a fundamental role in these experiments, by measuring the non–gravitational perturbations on MPO spacecraft and in effect being as much as possible the ideal test mass whose motion is tracked. ISA accelerometer, coming from a long research activity in fundamental physics and geophysics, will be the first one to fly on a deep–space mission, opening new research possibilities.

Acknowledgements. The authors wish to thank Roberto Formaro (ISA Program Manager, Agenzia Spaziale Italiana) and Thales Alenia Space. This research has made use of NASA's Astrophysics Data System.

References

Anselmi, A. & Scoon, G. E. N. 2001, Plan. Space Sci., 49, 1409

Benkhoff, J., van Casteren, J., Hayakawa, H., et al. 2010, Plan. Space Sci., 58, 2

Bruinsma, S., Loyer, S., Lemoine, J. M., Perosanz, F., & Tamagnan, D. 2003, J. Geod., 77, 86

Flury, J., Bettadpur, S., & Tapley, B. D. 2008, Adv. Space Res., 42, 1414

Iafolla, V., Fiorenza, E., Lefevre, C., et al. 2010, Plan. Space Sci., 58, 300

Iafolla, V., Lucchesi, D. M., Nozzoli, S., & Santoli, F. 2007, Celest. Mech. Dyn. Astron., 97, 165

Iafolla, V. & Nozzoli, S. 2001, Plan. Space Sci., 49, 1609

Lucchesi, D. M. & Iafolla, V. 2006, Celest. Mech. Dyn. Astron., 96, 99

Milani, A. & Gronchi, G. F. 2010, Theory of Orbit Determination (Cambridge: Cambridge University Press)

Milani, A., Rossi, A., Vokrouhlický, D., Villani, D., & Bonanno, C. 2001, Plan. Space Sci., 49, 1579

Milani, A., Vokrouhlický, D., Villani, D., Bonanno, C., & Rossi, A. 2002, Phys. Rev. D, 66, 082001

van den Ijssel, J. & Visser, P. 2007, Adv. Space Res., 39, 1597